

Ultrafast Carrier Dynamics in the Large Magnetoresistance Material WTe₂

Y. M. Dai,¹ J. Bowlan,¹ H. Li,² H. Miao,² Y. G. Shi,² S. A. Trugman,^{1,3} J.-X. Zhu,^{1,3} H. Ding,^{2,4} A. J. Taylor,¹ D. A. Yarotski,¹ and R. P. Prasankumar^{1,*}

¹*Center for Integrated Nanotechnologies, Los Alamos National Laboratory, Los Alamos, New Mexico 87545, USA*

²*Beijing National Laboratory for Condensed Matter Physics, Institute of Physics, Chinese Academy of Sciences, P.O. Box 603, Beijing 100190, China*

³*Theoretical Division, Los Alamos National Laboratory, Los Alamos, NM 87545, USA*

⁴*Collaborative Innovation Center of Quantum Matter, Beijing, China*

(Dated: October 22, 2019)

Ultrafast optical pump-probe spectroscopy is used to track carrier dynamics in the large magnetoresistance material WTe₂. Our experiments reveal a fast relaxation process occurring on a sub-picosecond time scale that is associated with electron-phonon thermalization. An additional slow relaxation process, occurring on a time scale of ~ 5 -15 picoseconds, is attributed to phonon-assisted electron-hole recombination. The timescale governing electron-hole recombination increases as the temperature is lowered down to ~ 50 K, below which it decreases continuously down to 5 K. This behavior results from competition between the reduction of interband electron-phonon scattering and the expansion of the hole pocket with decreasing temperature.

PACS numbers: 71.20.Be, 78.47.-p, 78.47.D-

The recent discovery of large positive magnetoresistance (MR) in a number of nonmagnetic materials such as WTe₂ [1], Cd₃As₂ [2] and NbSb₂ [3] has aroused tremendous interest, due not only to its potential application in devices such as magnetic sensors and hard drives, but also to the enigmatic nature of this effect. The observed MR in Cd₃As₂ has been attributed to the recovery of backscattering that is strongly suppressed in zero magnetic field [2]. In WTe₂, the large non-saturating MR is believed to arise from perfect electron-hole (e - h) compensation [1], similar to bismuth (Bi) and graphite [4–6]. This is supported by angle-resolved photoemission spectroscopy (ARPES) [7] and quantum oscillation [8] experiments, which have found hole and electron pockets with the same size in WTe₂ at low temperatures. Further support for the e - h compensation scenario came from the application of pressure, which increases the difference between the sizes of the hole and electron pockets, dramatically suppressing the MR [9–11]. However, a recent high resolution ARPES study revealed a more complicated Fermi surface (FS) with nine pockets [12]. In addition, circular dichroism was observed in their photoemission spectra, signaling strong spin-orbital coupling, which may also play an important role in WTe₂. Finally, a detailed study of the Shubnikov-de-Haas (SdH) effect, in combination with density functional theory (DFT) calculations, indicated that perfect e - h compensation breaks down under an external magnetic field in WTe₂ [13], challenging the e - h compensation scenario.

More insight into the physics of WTe₂ can be obtained using ultrafast optical spectroscopy, which tracks the relaxation of photoexcited carriers in the time domain as they return to equilibrium. Carrier relaxation depends sensitively on the band structure and scattering mechanisms in a solid [14–17], and therefore an understanding

of ultrafast carrier dynamics in WTe₂ may shed new light on the mechanism of the anomalous MR. However, ultrafast optical studies have not yet been performed on this material.

Here, we present a detailed ultrafast transient reflectivity [$\Delta R(t)/R$] study of WTe₂ while varying the temperature (T) and photoexcitation fluence (F). Two distinct relaxation processes contribute to the recovery of the photoinduced change in reflectivity. Electron-phonon (e - ph) thermalization is responsible for the fast decay that occurs on a sub-picosecond (ps) time scale, while e - h recombination between the electron and hole pockets occurs within ~ 5 -15 ps, giving rise to the slow decay in the $\Delta R(t)/R$ signal. The e - h recombination process gradually slows down upon cooling, but then becomes faster again below ~ 50 K. This anomalous T dependence of the e - h recombination time arises from competition between the reduction of e - ph scattering and the expansion of the hole pocket with decreasing temperature. The latter improves the e - h compensation and is likely an important factor in the emergence of the large MR.

High-quality WTe₂ single crystals were grown by solid-state reactions using Te as the flux. The starting materials W (99.9%) and excessive amounts of Te (99.999%) were mixed and placed in an alumina ampoule, then sealed in a quartz tube. The operation was in a glove box filled with high-purity argon gas. The temperature was increased to 1000°C over 10 h followed by heating the sample in a furnace at 1000°C for 5 h. After reaction, the system was cooled down to 800°C at a rate of 1°C/h, then to 700°C in 20 h. The quartz tube was then inverted and quickly spun in a centrifuge to remove the Te flux.

The transient reflectivity measurements were carried out using a Ti:sapphire femtosecond (fs) laser oscillator

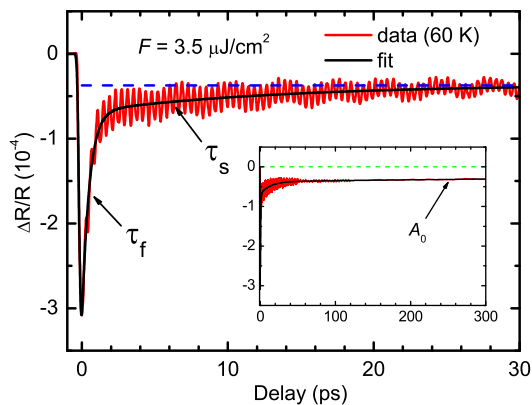


Figure 1. (color online) The transient reflectivity $\Delta R(t)/R$ (red line) as a function of time delay in WTe_2 at $T = 60$ K and $F = 3.5 \mu\text{J}/\text{cm}^2$. The black solid line shows the fit to the measured data, without including the oscillations. The dashed blue line shows the value of the $\Delta R(t)/R$ signal at long time delays, A_0 . The inset shows the $\Delta R(t)/R$ signal (red line) and the fitting result (black line) up to 300 ps.

producing pulses with a center wavelength of 830 nm (1.5 eV), a duration of 40 fs and a repetition rate of 80 MHz. The spot sizes of the pump and probe beams at the sample were ~ 65 and $32 \mu\text{m}$ in diameter, respectively. The pump fluence was tuned by a neutral density filter. For $F = 3.5 \mu\text{J}/\text{cm}^2$, using the optical properties at 830 nm [18], the photoexcited carrier density in WTe_2 is estimated to be $\sim 3.24 \times 10^{18} \text{cm}^{-3}$. Data was collected on a freshly cleaved surface from 5 to 300 K, with the pump and probe beams cross-polarized.

Figure 1 shows the $\Delta R(t)/R$ trace for WTe_2 at $T = 60$ K and $F = 3.5 \mu\text{J}/\text{cm}^2$. Photoexcitation results in a sharp drop in $\Delta R(t)/R$ due to the change in temperature of the electronic system after electron-electron ($e-e$) thermalization, followed by two distinct relaxation processes. A fast recovery of the photoinduced reflectivity change (τ_f) occurs within 1 ps, after which a slow decay (τ_s) with a weaker amplitude is observed. At longer time scales, the $\Delta R(t)/R$ signal is dominated by a flat offset (A_0), as shown in the inset of Fig. 1. In addition to these two decay processes, two oscillations with different frequencies are clearly observed in the $\Delta R(t)/R$ trace. These oscillations originate from the generation of coherent lattice vibrations by the femtosecond pump pulse [19, 20]. The frequencies of the two oscillations are 0.25 and 2.4 THz, respectively, agreeing well with the energies of two A_1 optical phonon modes in WTe_2 [21, 22].

In this Letter, we will focus on the non-oscillatory response, which provides pivotal information about the relaxation dynamics of photoexcited carriers in WTe_2 . In order to parameterize the experimental data, we fit the measured $\Delta R(t)/R$ signal to two exponential decays convoluted with a Gaussian function (representing the auto-

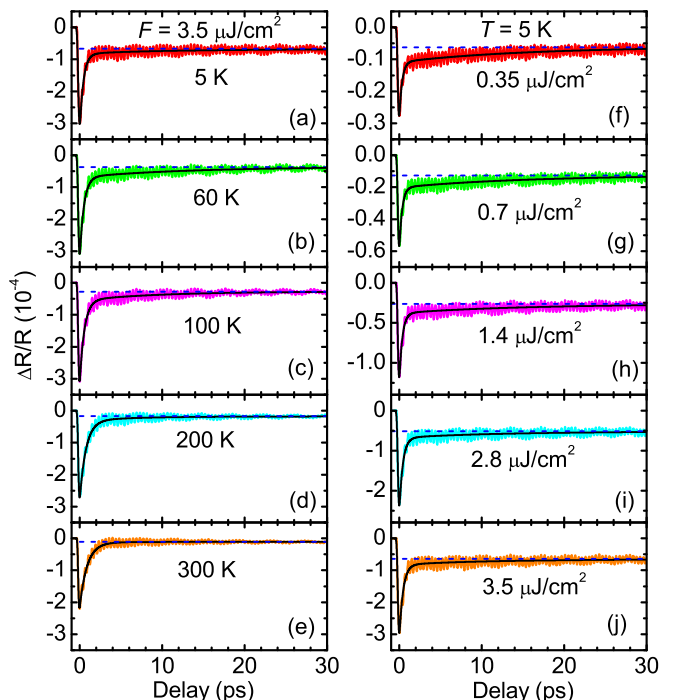


Figure 2. (color online) (a)–(e) $\Delta R(t)/R$ in WTe_2 at several selected temperatures between 5 and 300 K. The fluence of the pump pulse is $F = 3.5 \mu\text{J}/\text{cm}^2$. (f)–(j) $\Delta R(t)/R$ in WTe_2 measured with different pump fluences at 5 K. The black solid line through the data in each panel denotes the curve fit to the non-oscillatory response.

correlation of the pump and probe pulses). A_0 describes the flat offset at long time scales. This offset is usually related to heat diffusion out of the excitation volume on a timescale of several nanoseconds [23, 24], much longer than the measured timescale (300 ps). Therefore, we can reasonably take it as a constant.

To gain insight into the origin of the two relaxation processes, a careful examination of the T and F dependence of τ_f and τ_s is indispensable. Figures 2(a)–2(e) depict $\Delta R(t)/R$ at selected temperatures between 5 and 300 K. This reveals that τ_f becomes faster as the temperature is reduced; τ_s also exhibits noticeable T dependence, as can be seen by comparing the $\Delta R(t)/R$ curve with the blue dashed line (A_0) in each panel. In order to quantitatively study the T dependence of the two relaxation processes, we fit the $\Delta R(t)/R$ signal at all measured temperatures, returning the detailed T dependence of τ_f [Fig. 3(a)] and τ_s [Fig. 3(b)]. Figures 2(f)–2(j) show $\Delta R(t)/R$ measured with different fluences at 5 K. While τ_f is approximately F independent, τ_s becomes faster with increasing pump fluence. The decay rate for the slow component, $1/\tau_s$, extracted by fitting $\Delta R(t)/R$ to two exponential decays at each fluence, is plotted as a function of F in the inset of Fig. 3(b).

Having examined the T and F dependence of the two decays, we next trace their origins. In most materials,

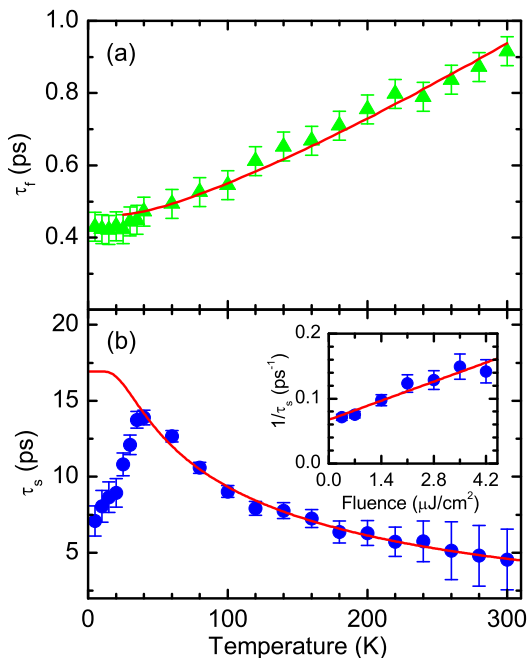


Figure 3. (color online) (a) and (b) show τ_f and τ_s , respectively, as a function of temperature for $F = 3.5 \mu\text{J}/\text{cm}^2$. The red solid curve denotes (a) the TTM fit and (b) the calculated T dependence of the phonon-assisted e - h recombination time, with a fixed density of states in the electron and hole Fermi pockets. The inset of (b) displays the decay rate $1/\tau_s$ as a function of the pump fluence, while the red solid line represents a linear fit to the data.

after femtosecond photoexcitation and e - e thermalization, which give rise to the initial sharp change in the $\Delta R(t)/R$ signal, the hot carriers transfer their excess energy to the lattice on a sub-ps time scale through e - ph interactions [24–26]. This makes it reasonable to attribute τ_f in WTe_2 to the cooling of the electronic system via e - ph thermalization. Further support comes from the T dependence of τ_f [Figure 3(a)], which is quite similar to the T -dependent e - ph thermalization time observed in other materials [19, 24, 26].

Electron-phonon thermalization is generally described by the two-temperature model (TTM) [15, 24, 25]. Within this model, the e - ph thermalization time τ_{e-ph} is given by [24, 26]

$$\tau_{e-ph} = \frac{\gamma(T_e^2 - T_l^2)}{2H(T_e, T_l)}, \quad (1)$$

where γ is the electron specific heat coefficient. T_e corresponds to the electron temperature after e - e thermalization, which is higher than the lattice temperature T_l . $H(T_e, T_l)$ takes the form

$$H(T_e, T_l) = f(T_e) - f(T_l), \quad (2)$$

where

$$f(T) = 4g_\infty \frac{T^5}{\theta_D^4} \int_0^{\theta_D/T} \frac{x^4}{e^x - 1} dx, \quad (3)$$

with θ_D and g_∞ denoting the Debye temperature and the e - ph coupling constant, respectively. T_e can be calculated using

$$T_e = \left(T_l^2 + \frac{2U_l}{\gamma} \right)^{1/2}, \quad (4)$$

where U_l is the deposited laser energy density. It is well known that the TTM is not an appropriate model for e - ph thermalization at low temperatures ($T \leq \theta_D/5$), where the e - e and e - ph thermalization times become comparable [15, 19, 26]. Since $\theta_D = 133.8$ K for WTe_2 [27], it is reasonable to use the TTM to describe e - ph thermalization above ~ 30 K. The red solid curve in Fig. 3(a) shows that the TTM fits the T dependence of τ_f (green solid triangles) quite well above 30 K. Using $U_l \simeq 0.78$ J/cm³, we can obtain the e - ph coupling constant and the electron specific heat coefficient from the TTM fit: $g_\infty \simeq 6.79 \times 10^{15}$ W m⁻³ K⁻¹ and $\gamma \simeq 0.81$ mJ mol⁻¹ K⁻². The good agreement of the TTM with our data supports our assignment of τ_f to e - ph thermalization.

The origin of the slow decay (τ_s) may be uncovered by examining the FS and electronic band structure of WTe_2 . DFT calculations [1, 28] have shown that both the valence and conduction bands barely cross the Fermi level at different points of the Brillouin zone, producing a pair of electron and hole pockets with equal size on each side of the Γ point in the Brillouin zone. This FS structure has been confirmed by ARPES [7] and quantum oscillation [8, 9] experiments. Interestingly, the ARPES study also shows that increasing the temperature leads to a dramatic shrinking of the hole pockets, degrading the e - h compensation [7]. A recent detailed ARPES measurement revealed a more complex FS [12]. Nevertheless, pairs of electron and hole pockets represent the dominant feature of the FS structure. Based on the above theoretical and experimental studies, a schematic band structure in the Γ - X direction for WTe_2 at low temperatures is traced out in Fig. 4, which will help us to understand the origin of τ_s .

After e - ph thermalization (τ_f) takes place (schematically illustrated in Fig. 4), there are still excess electrons (holes) in the conduction (valence) band. τ_s may therefore arise from e - h recombination between the conduction and valence bands. This could occur radiatively, as in semiconductors, where an electron in the conduction band can recombine with a hole in the valence band by emitting a photon [29]. However, this is unlikely to be the origin of τ_s in WTe_2 , because (i) radiative recombination usually occurs on a much longer time scale (a few nanoseconds) [29]; (ii) the emission of a photon can not

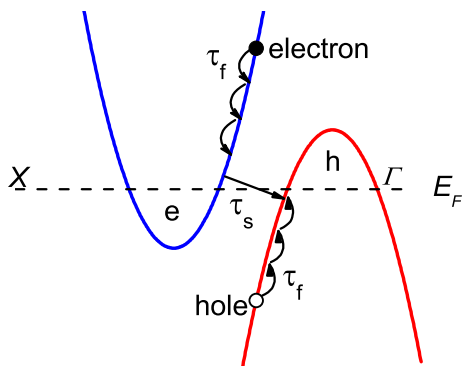


Figure 4. (color online) Schematic band structure of WTe_2 near the Fermi level (E_F) along the Γ - X direction at low temperatures. τ_f describes the e -ph thermalization process and τ_s represents the phonon-assisted interband e - h recombination process.

provide the momentum transfer needed for e - h recombination in WTe_2 . Alternatively, e - h recombination could occur via a three-body Auger process [30, 31], where an electron and a hole recombine and transfer the resulting energy to a third charge carrier. Nonetheless, (i) the T dependence of τ_s [Fig. 3(b)] does not favor Auger recombination, since this process is generally insensitive to temperature; (ii) the linear dependence of the decay rate $1/\tau_s$ on F , as shown in the inset of Fig. 3(b), is a clear signature of two-particle dynamics [14, 32]. Finally, we consider phonon-assisted e - h recombination, where the electron and hole recombine with the assistance of e -ph scattering between the electron and hole pockets, as illustrated by τ_s in Fig. 4. This has previously been observed and discussed in Bi [33, 34], a semimetal with a similar band structure to WTe_2 . The e - h recombination time in bismuth was found to be strongly T dependent and varies from a few to tens of ps [33, 34], in good agreement with the features of τ_s . Furthermore, we note that in WTe_2 , the conduction and valence band extrema are in close proximity within the Brillouin zone [1, 7], making interband e -ph scattering more favourable. These facts indicate that τ_s in WTe_2 may be due to phonon-assisted e - h recombination between the electron and hole pockets.

This assignment can also explain the anomalous T dependence of τ_s [Fig. 3(b)]. As the temperature is lowered from 300 K, τ_s first increases but then drops, resulting in a peak at about 50 K. A sharp change in the relaxation time constant often results from a phase transition [16, 35]. However, in WTe_2 , no phase transition has been reported at this temperature [1, 7, 8, 21, 27, 36], suggesting that the peak in the T dependence of τ_s is likely due to a crossover between competing mechanisms. A detailed theoretical calculation in graphene shows that the phonon-assisted e - h recombination time strongly depends on temperature and the electron and hole densi-

ties [37]. This calculation demonstrated that (i) the presence of more empty states in the valence band results in faster e - h recombination, since there are more holes for the photoexcited electrons to recombine with; (ii) lowering the temperature reduces the efficiency of interband e -ph scattering, leading to a longer e - h recombination time, because the phonon population is a strong function of temperature. In WTe_2 , at high temperatures, the hole pocket is small and the e - h compensation is relatively poor [7]. However, a large number of phonon modes are thermally excited, and the e - h recombination time may therefore be dominated by the interband e -ph scattering rate. Upon cooling, the phonon population diminishes and interband e -ph scattering becomes less effective, so that τ_s increases with decreasing temperature. In the presence of e -ph coupling, the T dependence of the phonon-assisted e - h recombination time, τ_R , can be quantitatively described using a model previously applied to phonon-assisted recombination in Bi [33]:

$$\frac{1}{\tau_R} = A \frac{\frac{\hbar\omega}{2kT}}{\sinh^2\left(\frac{\hbar\omega}{2kT}\right)} + \frac{1}{\tau_0}, \quad (5)$$

where ω corresponds to the frequency of the phonon mode assisting the e - h recombination; τ_0 represents a T -independent recombination time which varies with sample purity; A is a parameter related to the density of states in the conduction and valence bands and the matrix element for interband e -ph scattering. The red curve in Fig. 3(b) is the least-squares fit to the data using Eq. (5). The excellent agreement between the experimental data and the fitting result above 50 K is a strong indication that the e - h recombination time, τ_s , is dominated by interband e -ph scattering at high temperatures.

The discrepancy between the model and the experimental result below 50 K implies that at low temperatures, the e - h recombination time is governed by a different factor. In this temperature range, the efficiency of interband e -ph scattering is expected to be very low. However, the ARPES study in ref. [7] revealed that the hole pocket expands dramatically and the e - h compensation is significantly improved at low temperatures. The resulting large density of states created in the hole pocket can accelerate e - h recombination [37], causing τ_s to decrease below 50 K. In this context, the T dependence of τ_s is governed by the competition between the decreasing interband e -ph scattering rate and the expansion of the hole pocket with decreasing temperature.

Finally, a comparison between our results and other techniques may provide more insight into the anomalous MR in WTe_2 . The previous ARPES study [7] mapped the FSs at only two temperatures (20 and 100 K). Our ultrafast optical studies, carried out with more detailed T dependence, reveal a marked change in τ_s below ~ 50 K. This may indicate that the hole pocket expands more significantly below ~ 50 K. In addition, a sign change

in the thermoelectric power at ~ 60 K was reported in WTe_2 [36], which may also be relevant to the expansion of the hole pocket. Transport measurements [1, 38] have shown that the MR only turns on at low temperatures and increases sharply with decreasing temperature below ~ 50 K. Moreover, mass anisotropy, which reflects the FS structure, also increases rapidly below ~ 50 K, closely following the T dependence of the MR [38]. By connecting these results together, one may deduce that the expansion of the hole pocket, which improves the e - h compensation with decreasing temperature, plays an important role in enhancing the MR in WTe_2 . A more detailed investigation into the evolution of the Fermi surfaces with temperature will be highly informative in elucidating the origin of the large MR in WTe_2 .

In conclusion, we performed ultrafast transient reflectivity measurements on WTe_2 as a function of pump fluence and temperature. Two relaxation processes were clearly observed. We have ascribed the fast decay process to carrier cooling through e -ph thermalization and the slow decay process to phonon-assisted e - h recombination between the electron and hole bands. Competition between the reduction of interband e -ph scattering and the hole pocket expansion with decreasing temperature governs the T dependence of the recombination time. Finally, a comparison with other experimental results implies that the expansion of the hole pocket with decreasing temperature, which improves the e - h compensation, may play an important role in promoting the large MR in WTe_2 .

We thank Pamela Bowlan, Xia Dai, Jiangping Hu, Yongkang Luo, Brian McFarland, Kamaraju Natarajan, Ivo Pletikosić, Qiang Wang and Xianxin Wu for helpful discussions and especially thank Christopher C. Homes for sharing his unpublished optical data. This work was performed at the Center for Integrated Nanotechnologies, a U.S. Department of Energy, Office of Basic Energy Sciences user facility. Los Alamos National Laboratory, an affirmative action equal opportunity employer, is operated by Los Alamos National Security, LLC, for the National Nuclear Security administration of the U.S. Department of Energy under contract no. DE-AC52-06NA25396. Work at LANL was supported by the LANL LDRD program and by the UC Office of the President under the UC Lab Fees Research Program, Grant ID No. 237789. Work at IOP CAS was supported by the Strategic Priority Research Program (B) of the Chinese Academy of Sciences (Grant No. XDB07020100) and the National Natural Science Foundation of China (No. 11274367, 11474330).

* rpprasan@lanl.gov

[1] M. N. Ali, J. Xiong, S. Flynn, J. Tao, Q. D. Gib-

- son, L. M. Schoop, T. Liang, N. Haldolaarachchige, M. Hirschberger, N. P. Ong, et al., *Nature* **514**, 205 (2014).
- [2] T. Liang, Q. Gibson, M. N. Ali, M. Liu, R. J. Cava, and N. P. Ong, *Nat. Mater.* **14**, 280 (2015).
- [3] K. Wang, D. Graf, L. Li, L. Wang, and C. Petrovic, *Sci. Rep.* **4**, 07328 (2014).
- [4] P. B. Alers and R. T. Webber, *Phys. Rev.* **91**, 1060 (1953).
- [5] F. Y. Yang, K. Liu, K. Hong, D. H. Reich, P. C. Searson, and C. L. Chien, *Science* **284**, 1335 (1999).
- [6] X. Du, S.-W. Tsai, D. L. Maslov, and A. F. Hebard, *Phys. Rev. Lett.* **94**, 166601 (2005).
- [7] I. Pletikosić, M. N. Ali, A. V. Fedorov, R. J. Cava, and T. Valla, *Phys. Rev. Lett.* **113**, 216601 (2014).
- [8] Z. Zhu, X. Lin, J. Liu, B. Fauqué, Q. Tao, C. Yang, Y. Shi, and K. Behnia, *Phys. Rev. Lett.* **114**, 176601 (2015).
- [9] P. L. Cai, J. Hu, L. P. He, J. Pan, X. C. Hong, Z. Zhang, J. Zhang, J. Wei, Z. Q. Mao, and S. Y. Li, arXiv:1412.8298 (2014).
- [10] D. Kang, Y. Zhou, W. Yi, C. Yang, J. Guo, Y. Shi, S. Zhang, Z. Wang, C. Zhang, S. Jiang, et al., arXiv:1502.00493 (2015).
- [11] X.-C. Pan, X. Chen, H. Liu, Y. Feng, F. Song, X. Wan, Y. Zhou, Z. Chi, Z. Yang, B. Wang, et al., arXiv:1501.07394 (2015).
- [12] J. Jiang, F. Tang, X. C. Pan, H. M. Liu, X. H. Niu, Y. X. Wang, D. F. Xu, H. F. Yang, B. P. Xie, F. Q. Song, et al., arXiv:1503.01422 (2015).
- [13] D. Rhodes, S. Das, Q. R. Zhang, B. Zeng, N. R. Pradhan, N. Kikugawa, E. Manousakis, and L. Balicas, arXiv:1505.01242 (2015).
- [14] D. H. Torchinsky, G. F. Chen, J. L. Luo, N. L. Wang, and N. Gedik, *Phys. Rev. Lett.* **105**, 027005 (2010).
- [15] J. Demsar, R. D. Averitt, K. H. Ahn, M. J. Graf, S. A. Trugman, V. V. Kabanov, J. L. Sarrao, and A. J. Taylor, *Phys. Rev. Lett.* **91**, 027401 (2003).
- [16] E. E. M. Chia, D. Talbayev, J.-X. Zhu, H. Q. Yuan, T. Park, J. D. Thompson, C. Panagopoulos, G. F. Chen, J. L. Luo, N. L. Wang, et al., *Phys. Rev. Lett.* **104**, 027003 (2010).
- [17] J. Qi, T. Durakiewicz, S. A. Trugman, J.-X. Zhu, P. S. Riseborough, R. Baumbach, E. D. Bauer, K. Gofryk, J.-Q. Meng, J. J. Joyce, et al., *Phys. Rev. Lett.* **111**, 057402 (2013).
- [18] C. C. Homes, M. N. Ali, and R. J. Cava, arXiv:1506.02599 (2015).
- [19] M. Hase, K. Ishioka, J. Demsar, K. Ushida, and M. Kitajima, *Phys. Rev. B* **71**, 184301 (2005).
- [20] J. Qi, X. Chen, W. Yu, P. Cadden-Zimansky, D. Smirnov, N. H. Tolk, I. Miotkowski, H. Cao, Y. P. Chen, Y. Wu, et al., *Appl. Phys. Lett.* **97**, 182102 (2010).
- [21] W.-D. Kong, S.-F. Wu, P. Richard, C.-S. Lian, J.-T. Wang, C.-L. Yang, Y.-G. Shi, and H. Ding, *Appl. Phys. Lett.* **106**, 081906 (2015).
- [22] Y. Jiang and J. Gao, arXiv:1501.04898 (2015).
- [23] C. W. Luo, I. H. Wu, P. C. Cheng, J.-Y. Lin, K. H. Wu, T. M. Uen, J. Y. Juang, T. Kobayashi, D. A. Chareev, O. S. Volkova, et al., *Phys. Rev. Lett.* **108**, 257006 (2012).
- [24] L. Cheng, C. La-o-vorakiat, C. S. Tang, S. K. Nair, B. Xia, L. Wang, J.-X. Zhu, and E. E. M. Chia, *Appl. Phys. Lett.* **104**, 211906 (2014).
- [25] P. B. Allen, *Phys. Rev. Lett.* **59**, 1460 (1987).

- [26] R. H. M. Groeneveld, R. Sprik, and A. Lagendijk, *Phys. Rev. B* **51**, 11433 (1995).
- [27] J. E. Callanan, G. Hope, R. D. Weir, and E. F. W. Jr., *J. Chem. Thermodyn.* **24**, 627 (1992).
- [28] J. Augustin, V. Eyert, T. Böker, W. Frentrup, H. Dwelk, C. Janowitz, and R. Manzke, *Phys. Rev. B* **62**, 10812 (2000).
- [29] A. Othonos, *Journal of Applied Physics* **83**, 1789 (1998).
- [30] K. L. Vodopyanov, H. Graener, C. C. Phillips, and T. J. Tate, *Phys. Rev. B* **46**, 13194 (1992).
- [31] Y. Onishi, Z. Ren, K. Segawa, W. Kaszub, M. Lorenc, Y. Ando, and K. Tanaka, *Phys. Rev. B* **91**, 085306 (2015).
- [32] G. P. Segre, N. Gedik, J. Orenstein, D. A. Bonn, R. Liang, and W. N. Hardy, *Phys. Rev. Lett.* **88**, 137001 (2002).
- [33] A. A. Lopez, *Phys. Rev.* **175**, 823 (1968).
- [34] Y. M. Sheu, Y. J. Chien, C. Uher, S. Fahy, and D. A. Reis, *Phys. Rev. B* **87**, 075429 (2013).
- [35] J. Demsar, B. Podobnik, V. V. Kabanov, T. Wolf, and D. Mihailovic, *Phys. Rev. Lett.* **82**, 4918 (1999).
- [36] S. Kabashima, *J. Phys. Soc. Jpn.* **21**, 945 (1966).
- [37] F. Rana, P. A. George, J. H. Strait, J. Dawlaty, S. Shivaraman, M. Chandrashekar, and M. G. Spencer, *Phys. Rev. B* **79**, 115447 (2009).
- [38] L. R. Thoutam, Y. L. Wang, Z. L. Xiao, S. Das, A. Luican-Mayer, R. Divan, G. W. Crabtree, and W. K. Kwok, arXiv:1506.02214 (2015).